Axial form factors of the nucleon

Sara Collins

Universität Regensburg

Lattice@CERN 2024, July 17th 2024

Motivation: neutrino oscillation experiments

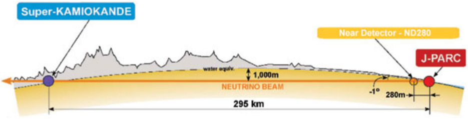

T2K: Tokai to Super-Kamiokande,

$E = 0.6$ GeV, $L/E \approx 500$ **km/GeV.**

Also NOvA, $L/E \approx 400$ km/GeV, DUNE $L/E \approx 520$ km/GeV, HK(=T2K).

Muon neutrino beam: proton on nucleus $\to$ pions and kaons $\to \mu^+\nu_\mu$ or $\mu^-\bar{\nu}_\mu$.

Near and far detectors.

$$\mathbf{N}^{\mu}_{\text{far}}(\mathbf{E}_\nu) = \mathbf{N}^{\mu}_{\text{near}}(\mathbf{E}_\nu) \times [\text{flux(L)}] \times [\text{detector}] \times [1 - \sum_\beta \mathbf{P}_{\mu\to\beta}(\mathbf{E}_\nu)]$$

E_ν has to be reconstructed from the momentum of the detected charged lepton.

$\nu_\mu + n \to \mu^- + p$

But. . .
The neutrino beam is not monochromatic but has a momentum distribution.
The nucleon is bound in a nucleus and has $|\mathbf{p}_{\text{Fermi}}| \sim 200\,\text{MeV}$.
The lepton momentum reconstruction is often incomplete.
Misidentification of inelastic scattering as elastic scattering.

Monte-Carlo simulation needs input regarding the differential cross section.

Neutrino-nucleon scattering cross-section

Quasi-elastic scattering (QE)

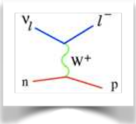

Resonance production (RES)

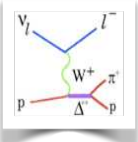

Deep Inelastic scattering (DIS)

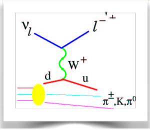

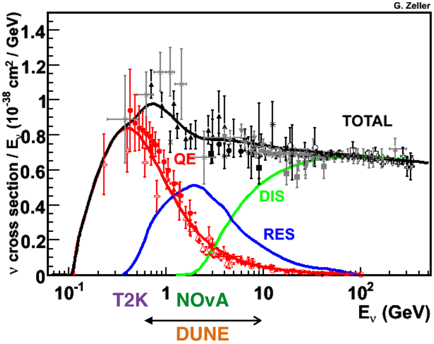

J.A. Formaggio, G. Zeller, Reviews of Modern Physics, 84 (2012)

Overview: Quasi-elastic scattering (axial form factors), excited state contamination.
Steps towards $N \to N\pi$ matrix elements.

Quasi-elastic scattering

Relevant $V - A$ matrix element in the isospin limit:

$$\langle \mathbf{p}(\mathbf{p}')|\bar{\mathbf{u}}\gamma_\mu(\mathbf{1}-\gamma_5)\mathbf{d}|\mathbf{n}(\mathbf{p})\rangle = \overline{u}_p(p')\left[\gamma_\mu \boldsymbol{F_1(Q^2)} + \frac{i\sigma_{\mu\nu}q^\nu}{2m_N}\boldsymbol{F_2(Q^2)}\right.$$
$$\left. + \gamma_\mu\gamma_5 \boldsymbol{G_A(Q^2)} + \frac{q^\mu}{2m_N}\gamma_5 \boldsymbol{\tilde{G}_P(Q^2)}\right] u_n(p)$$

$q_\mu = p'_\mu - p_\mu$, virtuality $Q^2 = -q^2 > 0$.

Dirac and Pauli form factors $F_{1,2}$ are reasonably well determined experimentally from lepton-nucleon scattering for range of $Q^2 \sim (0.1-1)$ GeV^2 relevant for the long-baseline experiments.

Axial form factor: forward limit: $G_A(Q^2) \to g_A$ (well determined from β-decay).

Shape at low Q^2, $\langle r_A^2\rangle = -6\frac{dG_A(Q^2)}{dQ^2}$:

$$G_A(Q^2) = G_A(0)\left[1 - \frac{1}{6}\langle r_A^2\rangle Q^2 + \ldots\right]$$

Parameterisation: dipole form $G_A(q^2) = \frac{g_A}{(1+\frac{q^2}{\mathbf{M_A}^2})^2}$, $M_A = 12/\langle r_A^2\rangle^{1/2}$, z-expansion.

Axial and induced pseudoscalar form factors

$G_A(Q^2)$: information from old $\bar{\nu}$-p and ν-d scattering data.

Over-constrained dipole fits performed: e.g. [Bernard et al.,hep-ph/0107088]
$M_A = 1.03(2)$ GeV.

z-expansion analysis from [Meyer,1603.03048] $M_A = 1.01(24)$ **GeV**.

Neutrino scattering with nuclear targets, e.g. [MiniBooNE,1002.2680] $M_A = 1.35(17)$ GeV (using the dipole form).

$\tilde{G}_P(Q^2)$:

Impact on the cross section is suppressed by a factor $m_\ell^2/m_N^2 \approx 0.01$ for $\ell = \mu$.

Only relevant for very small Q^2, where this formfactor is large.

Not well constrained: experimentally measured at the muon capture point. In muonic hydrogen, $\mu^- + p \to \nu_\mu n$.

[MuCAP, 1210.6545] : $g_P^* = m_\mu \tilde{G}_P(0.88 m_\mu^2)/(2m_N) = 8.06 \pm 0.48 \pm 0.28.$

Additional indirect information on G_A and $\tilde{G}_P$ via low energy theorems from pion electroproduction $e^- + N \to \pi + N + e^-$.

PCAC relation and pion pole dominance

For nucleon matrix elements: $A_\mu = \bar{u}\gamma_\mu\gamma_5 d$, $P = \bar{u}i\gamma_5 d$.

$$\mathbf{2\,m_q}\langle N(\vec{p}\,')|\mathbf{P}|N(\vec{p})\rangle = \langle N(\vec{p}\,')|\partial_\mu \mathbf{A}_\mu|N(\vec{p})\rangle + \mathcal{O}(a^2)$$

leads to

$$m_q G_P(Q^2) = m_N G_A(Q^2) - \frac{Q^2}{4m_N}\tilde{G}_P(Q^2)$$

where the **pseudoscalar form factor**: $\langle p(p')|P|n(p)\rangle = \overline{u}_p i\gamma_5 \boldsymbol{G_P(Q^2)} u_n$.

SU(2) chiral limit: $\tilde{G}_P(Q^2) = 4m_N^2 G_A(Q^2)/Q^2$

Pion pole dominance (LO ChPT): only an approximation.

$$\tilde{G}_P(Q^2) = G_A(Q^2)\frac{4m_N^2}{Q^2 + m_\pi^2} + \text{corrections}$$

PCAC+pion pole dominance (PPD) $\rightarrow$ one independent form factor

$$G_P(Q^2) = G_A(Q^2)\frac{m_N}{m_\ell}\frac{m_\pi^2}{Q^2 + m_\pi^2} + \text{corrections}$$

Lattice details:

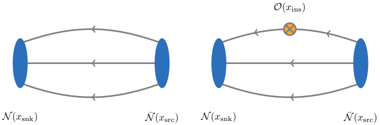

Three-point functions are evaluated with the sequential source method [Martinelli,Sachrajda,(1989)].

For each t, $t > \tau > 0$. Choose $\vec{p}' = \vec{0}$ with $\vec{p} = -\vec{q}$.

Extra propagator inversion for every sink t.

Spectral decomposition:

$$C_{2pt}^{\vec{p}}(t) = \boldsymbol{Z_{\vec{p}} Z^*_{\vec{p}}} \frac{E_{\vec{p}} + m_N}{E_{\vec{p}}} e^{-E_{\vec{p}} t} \left[1 + b_1 e^{-t\boldsymbol{\Delta_{\vec{p}}}} + \ldots\right]$$

Overlap factors: $\boldsymbol{Z_{\vec{p}}} u_N(\vec{p}) = \langle 0|\mathcal{N}|N(\vec{p})\rangle$, $b_1 \propto |\boldsymbol{Z^1_{\vec{p}}}|^2/|\boldsymbol{Z_{\vec{p}}}|^2$.

Energy difference between first excited and ground state: $\boldsymbol{\Delta_{\vec{p}}} = E^1_{\vec{p}} - E_{\vec{p}}$.

$$C_{3pt,\Gamma_i}^{\vec{p}',\vec{p},J}(t,\tau) = \frac{\boldsymbol{Z_{\vec{p}'} Z^*_{\vec{p}}}}{2E_{\vec{p}'} 2E_{\vec{p}}} e^{-E_{\vec{p}'}(t-\tau)} e^{-E_{\vec{p}}\tau} \boldsymbol{B^{\vec{p}',\vec{p}}_{\Gamma_i,J}}$$
$$\cdot \left[1 + c_{10} e^{-(t-\tau)\boldsymbol{\Delta_{\vec{p}'}}} + c_{01} e^{-\tau\boldsymbol{\Delta_{\vec{p}}}} + c_{11} e^{-(t-\tau)\boldsymbol{\Delta_{\vec{p}'}}} e^{-\tau\boldsymbol{\Delta_{\vec{p}}}} \ \ldots\right]$$

where $\boldsymbol{B^{\vec{p}',\vec{p}}_{\Gamma_i,J}} \propto \boldsymbol{\langle N|J|N\rangle}$, $c_{10} \propto \langle N_1|J|N\rangle$, $c_{01} \propto \langle N|J|N_1\rangle$, $c_{11} \propto \langle N_1|J|N_1\rangle$.
Smeared interpolators reduce $|\boldsymbol{Z^1_{\vec{p}}}|^2/|\boldsymbol{Z_{\vec{p}}}|^2$, however, $\langle N|J|N_1\rangle$ etc may be large.

Challenges

Statistical noise: signal vs noise decays with $e^{-(E-3m_\pi/2)t}$ for large t.

$\vec{p} = \vec{0}$

[NME,2103.05599]

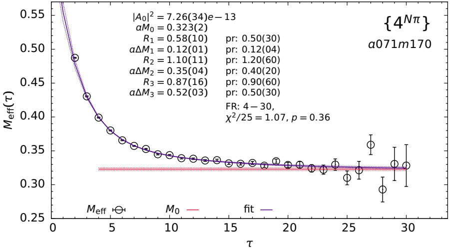

[Mainz,2212.09940]

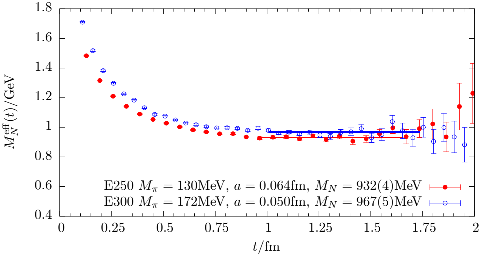

NME: 1 fm $\sim 14a$.

Wuppertal (Gaussian) smearing of nucleon interpolators using APE smeared gauge transporters.

NME: $\langle r^2\rangle^{1/2}_{\psi^2} \sim 0.76$ fm, Mainz: $\langle r^2\rangle^{1/2}_{\psi^2} \sim 0.50$ fm.

Challenges

Excited state pollution: significant since t in $C^N_{3pt}(t,\tau)$ cannot be too large.

Spectrum contains resonances and **multi-particle states**. Latter will be lowest excitations for ensembles with pion masses close to m_π^{phys} and $Lm_\pi \gtrsim 4$.

Source: $\vec{p} \neq 0$, parity not a good QN, $\boldsymbol{N(\vec{p})\pi(\vec{0})}$, $N(\vec{0})\pi(\vec{p})$, ...

Sink: $\vec{p}' = \vec{0}$, parity is a good QN, $\boldsymbol{N(\vec{p})\pi(-\vec{p})}$, $N(\vec{0})\pi(\vec{0})\pi(\vec{0})$ and $N\pi\pi\pi$ etc + momentum combinations.

CLS ensembles:

$m_\pi = 286$ MeV, $a = 0.064$ fm.

Forward limit: $C_{3pt}(t,\tau)/C_{2pt}(t) \to g_A$.

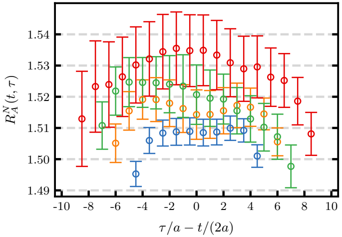

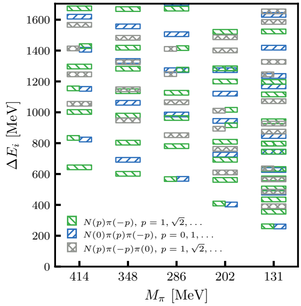

Assume for $Lm_\pi \gtrsim 4$: $E_{N\pi} \approx E_N + E_\pi$.

Challenges

Additional systematics to be controlled.

⋆ **Discretisation effects**: $\mathcal{O}(a)$ or $\mathcal{O}(a^2)$. More important as $\vec{p}$ becomes large.

⋆ **Quark mass dependence**: not clear how well ChPT describes the quark mass dependence in the range $m_\pi \sim (m_\pi^{phys} - 300\ \text{MeV})$.

E.g. NNLO SU(2) covariant BChPT [Schindler et al.,nucl-th/0611083]

$$G_A(0) \equiv g_A = g_A^{(0)} + g_A^{(1)} m_\pi^2 + g_A^{(2)} m_\pi^2 \ln\left(\frac{m_\pi}{\mu}\right) + g_A^{(3)} m_\pi^3$$

In ChPT, the $g_A^{(2)}$ log term gives a large positive contribution.

Lattice results find a mild dependence on m_π with a negative slope, large cancellation between terms.

The Δ resonance also needs to be considered.

Need $m_\pi \approx m_\pi^{phys}$.

⋆ **Finite volume effects**: exponentially suppressed $\sim m_\pi^2 e^{-Lm_\pi}/(m_\pi L)^{3/2}$, want $Lm_\pi \gtrsim 4$.

⋆ Parameterisation of Q^2 dependence.

Recent progress

Statistical noise and excited state pollution:

More source-sink separations, $t_{max} = 1.4 - 1.6$ fm. More measurements for larger t.

[ETMC,2309.05774] $m_\pi = 140$ MeV, $a = 0.09$ fm

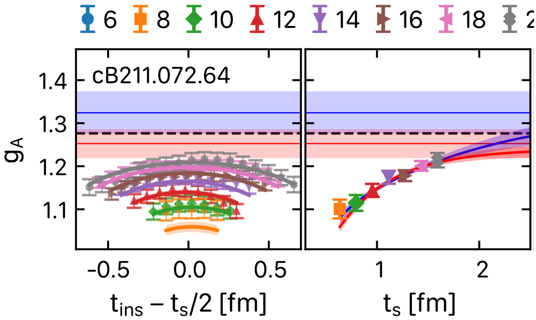

cB211.072.64		
750 configurations		
t_s/a	t_s[fm]	n_{src}
8	0.64	1
10	0.80	2
12	0.96	5
14	1.12	10
16	1.28	32
18	1.44	112
20	1.60	128

[Mainz,2207.03440]: $m_\pi = 129$ MeV, $t_{max} = 1.4$ fm, 102k measurements on 400 configs..
[PNDME,2305.11330]: $m_\pi = 128$ MeV, $t_{max} = 1.4$ fm, 170k measurements on 1290 configs..

Both Mainz and PNDME use TSM/AMA [Bali et al.,0910.3970], [Blum et al.,1208.4349].

Systematics from finite a and V and m_q dependence: most studies 3-5 lattice spacings, $m_\pi^{min} \approx m_\pi^{phys}$ and $Lm_\pi^{min} \gtrsim 3.5$.

Forward limit: axial charge, $G_A(0) \equiv g_A$

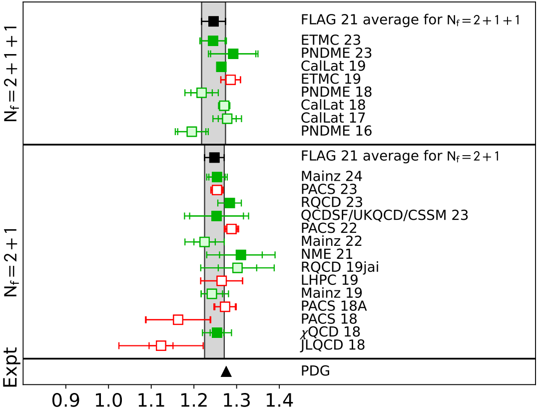

Not a FLAG plot, however, the FLAG criteria are applied.

ETMC 23, PNDME 23, Mainz 22 and RQCD 19 results obtained from data for $Q^2 > 0$ as well as $Q^2 = 0$.

Rest: $Q^2 = 0$ only.

PCAC relation: $\partial^\mu A_\mu = 2m_\ell P + \mathcal{O}(a^2)$

m_q extracted using **pion two-point correlation functions**:

zero momentum : $$\mathbf{2m_\ell} = \frac{\partial_t \langle A_4(t) P^\dagger(0)\rangle}{\langle P(t) P^\dagger(0)\rangle} = \frac{\partial_t C_{2pt}^{PA_4}(t)}{C_{2pt}^{PP}(t)}$$

Using **nucleon three-point correlation functions**:

finite $\vec{q}$: $$\mathbf{2m_\ell} = \frac{\langle \mathcal{N}_{snk} \partial_\mu A_\mu(x) \overline{\mathcal{N}}_{src}\rangle}{\langle \mathcal{N}_{snk} P(x) \overline{\mathcal{N}}_{src}\rangle} = \frac{\partial_\mu C_{3pt,P_i}^{\vec{0},\vec{p},A_\mu}(t,\tau)}{C_{3pt,P_i}^{\vec{0},\vec{p},P}(t,\tau)}$$

[RQCD,1810.05569]

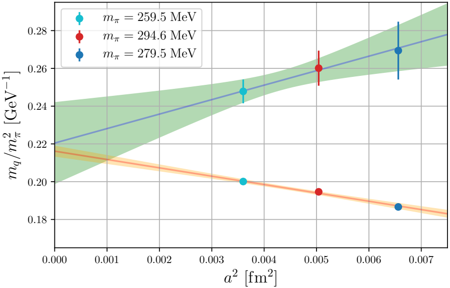

PCAC relation

$$\mathbf{r_{PCAC}} = \frac{m_q G_P(Q^2) + \frac{Q^2}{4m_N}\tilde{G}_P(Q^2)}{m_N G_A(Q^2)} = 1 + \mathbf{O(a^2)} \qquad r_{PPD} = \frac{m_\pi^2 + Q^2}{4m_N^2}\frac{\tilde{G}_P(Q^2)}{G_A(Q^2)} = 1 + \ldots$$

[Jang et al.,1905.06470]

$m_\pi \sim m_\pi^{phys}$, $a = 0.09$ fm.

Circles: excited state spectrum extracted from C_{2pt} and used in fit of C_{3pt}.

Lowest $N\pi$ state(s) not resolved in C_{2pt}. Size of excited state contributions underestimated.

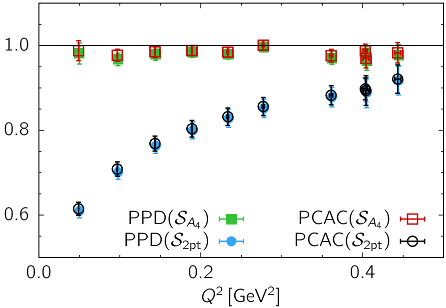

Discrepancy biggest for low Q^2 and $m_\pi \to m_\pi^{phys}$.

No improvement with smaller a, see, e.g., [RQCD,1911.13150].

Excited state contamination

$m_\pi = 200$ MeV, $a = 0.064$ fm, $|\vec{q}| = 2\pi/(64a)$ [RQCD,1911.13150]

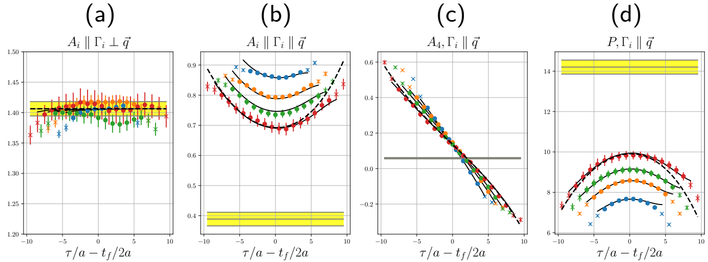

$$R_{\mathcal{J},\Gamma_i,\vec{q}} = C^{\vec{p}',\vec{p},J}_{3pt,\Gamma_i} / C^{\vec{p}}_{2pt} \times \text{(factor)} \to \text{constant}$$

$(a)\ R_{A_i\parallel\Gamma_i\perp\vec{q}} \propto G_A(Q^2)$

$(b)\ R_{A_i\parallel\Gamma_i\parallel\vec{q}} \propto (m_N + E_{\vec{q}})G_A(Q^2) - \dfrac{q_i^2}{2m_N}\tilde{G}_P(Q^2)$

$(c)\ R_{A_4,\Gamma_i\parallel\vec{q}} \propto G_A(Q^2) + \dfrac{(m_N - E_{\vec{q}})}{2m_N}\tilde{G}_P(Q^2)$

$(d)\ R_{P,\Gamma_i\parallel\vec{q}} \propto G_P(Q^2)$

Well known problem: e.g. [RQCD,1412.7336], [ETMC,1705.03399], [PNDME,1705.06834], [RQCD,1810.05569], [PACS,1811.07292].

Some works only extract G_A, using $R_{A_i\parallel\Gamma_i\perp\vec{q}}$.

Excited state contamination in ChPT

$N\pi$ excited state contamination in correlation functions can be investigated in ChPT.

For example,

Forward limit (zero recoil):
[Tiburzi,0901.0657,1503.06329] $N\pi$ excited state contribution to $G_A(0) = g_A$ in leading loop order HBChPT.
[Hansen,1610.03843] $N\pi$ excited state contribution to g_A, LO ChPT with finite volume interaction corrections a la Lellouch-Lüscher.
[Bär,1606.09385] BChPT: leading loop order g_A.

Form factors:
[Meyer,1811.03360] $N\pi$ contributions to $G_A(Q^2)$, $\tilde{G}_P(Q^2)$ and $G_P(Q^2)$ computed to tree-level in ChPT.
[Bär,1906.03652,1812.09191] $N\pi$ contributions to $G_A(Q^2)$, $\tilde{G}_P(Q^2)$ and $G_P(Q^2)$ computed in leading loop order BChPT.

Limitations to ChPT approach: p and m_π should be small. Applies to large source-sink separation (not always accessible due to deterioration of the signal). When using spatially extended sources $\langle r^2\rangle^{1/2}_{smear} \ll 1/m_\pi$.

Excited state contamination in ChPT

Ground state (single particle): $N(-\vec{q}) \to N(\vec{0})$.

Axial and pseudoscalar currents can couple to pions: dominant contributions come from **tree-level diagrams**, where the pion takes the momentum of the current:

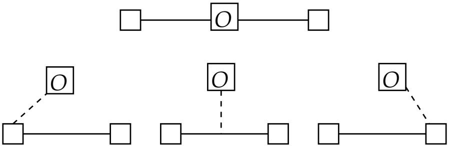

Top (ground state), bottom middle (ground+excited states), rest (excited states).

Channels $\mathcal{J} = \mathcal{P}$, $\mathcal{A}_4$ and $\mathcal{A}_i \parallel \vec{q}$: large $N(\vec{0})\pi(-\vec{q}) \to N(\vec{0})$ and $N(-\vec{q}) \to N(-\vec{q})\pi(\vec{q})$ contributions.

Only extraction of G_P and $\tilde{G}_P$ affected.

$\mathcal{J} = \mathcal{A}_i \parallel \vec{q}$: correction to $\tilde{G}_P(t, \tau = t/2) \sim -e^{-E_\pi(\vec{q})t/2}$ for small $\vec{q}$. [Bär,1906.03652]

No enhanced excited state contributions to G_A.

$\to$ (moderate) loop contributions to $\mathcal{A}_i \perp \vec{q}_i$.

No enhanced contributions in the forward limit. Consistent with the lattice data.

Excited state fits accounting for $N\pi$ states

[Jang et al.,1905.06470]

Expected first excitation: $\vec{p} = \vec{n}\frac{2\pi}{L}$

Sink: $N(-\vec{p})\pi(\vec{p})$

Source: $N(0)\pi(\vec{p})$

Fit to C_{3pt}: **first fix excited state energy from A_4 component.** Additional excited states also considered. See also [PNDME,2305.11330].

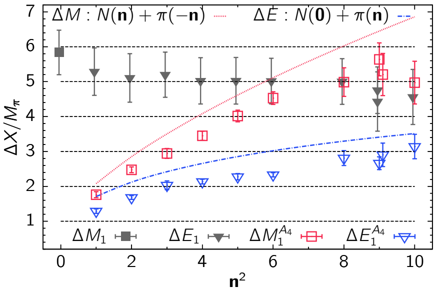

[RQCD,1911.13150]: **use tree-level BChPT to determine form of $N\pi$ contributions.** No constraints on the ground state contributions.

$$C_{3pt}^{\Gamma_\alpha, A_\mu}(\vec{p}\,', \vec{p}, t_f, \tau) = \frac{\sqrt{Z_{\vec{p}\,'} Z_{\vec{p}}}}{2E_{\vec{p}\,'} E_{\vec{p}}} e^{-E_{\vec{p}\,'}(t_f-\tau)} e^{-E_{\vec{p}}\tau} \times$$

$$\left[\boldsymbol{B_{\Gamma_i, A_\mu}(\vec{p}\,', \vec{p})} + \frac{E_{\vec{p}\,'}}{E_\pi} r_+^\mu c^{\vec{p}\,'} q_\alpha e^{-\Delta E^{N\pi}_{\vec{p}\,'}(t-\tau)} + \frac{E_{\vec{p}}}{E_\pi} r_-^\mu c^{\vec{p}} q_\alpha e^{-\Delta E^{N\pi}_{\vec{p}}(\tau)} + \ldots \right]$$

Energy gaps $\Delta E^{N\pi}_{\vec{p}\,'}$ and $\Delta E^{N\pi}_{\vec{p}}$ fixed using priors in the fit.

Second excited state included in the fit with the standard form.

$N\pi$ terms for $C_{3pt}^{\Gamma_\alpha, P}$ obtained from the PCAC relation.

Simultaneous fit of C_{3pt} for the A_μ and P currents gives a reasonable χ^2/dof.

Recent works with $m_\pi \to m_\pi^{phys}$, $V \to \infty$, $a \to 0$ limits

[ETMC,2309.05774] $N_f = 2+1+1$, $a = 0.08, 0.07, 0.06$ fm, $m_\pi \sim m_\pi^{phys}$, $Lm_\pi = 3.6 - 3.9$.

Simultaneous fits to C_{2pt} and C_{3pt} for the A_μ and P currents. One and two excited state contributions explored (final results from the one excited state fit difference included in the systematics).

Q^2 parameterisation and $a \to 0$ limit:

$$G_z(Q^2, a^2) = g(a^2) \sum_{k=0}^{k_{max}} c_k(a^2) z^k(Q^2) \qquad z(t, t_{cut}, t_0) = \frac{\sqrt{t_{cut} - t} - \sqrt{t_{cut} - t_0}}{\sqrt{t_{cut} - t} + \sqrt{t_{cut} - t_0}}$$

$t = q^2 = -Q^2$, $t_{cut} = 9m_\pi^2$, $k_{max} = 3$, $t_0 = 0$.

Coefficients constrained by restrictions that expansion converges smoothly to zero as $Q^2 \to \infty$ following [Lee et al.,1505.01489], [Meyer et al.,1603.03048].

For $\tilde{G}_P$ and $G'_P = 4m_N/m_\pi^2 \times m_q G_P(Q^2)$ use: $G_{wpole}(Q^2, a^2) = \frac{1}{Q^2 + m_\pi^2 + ba^2} G_z(Q^2, a^2)$

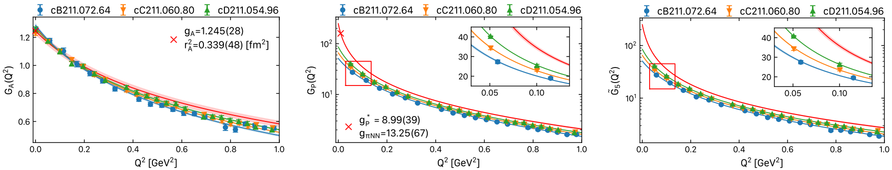

Recent works with $m_\pi \to m_\pi^{phys}$, $V \to \infty$, $a \to 0$ limits

[RQCD,1911.13150]: $N_f = 2+1$ $O(a)$-improved Wilson ensembles (CLS), 5 lattice spacings, $a = 0.09 - 0.04$ fm, $m_\pi = 130 - 410$ MeV, $Lm_\pi^{phys} = 3.5 - 4.1$.

Simultaneous fit to $\mathcal{J} = \mathcal{A}_\mu$ and $\mathcal{P}$ C_{3pt}/C_{2pt} functions (two excited states, first set to $E_{N\pi}$). Four source-sink separations $t = 0.7 - 1.2$ fm.

Combined m_q, V, a^2 and Q^2 (z-expansion) fit of G_A, $\tilde{G}_P$, G_P (after testing in the continuum limit, the PCAC relation imposed).

Constraints on coefficients from asymptotic behaviour $G_A \propto 1/Q^4$ etc. and the PCAC relation. $k_{max} = 4 + 3$.

[PNDME,2305.11330]: clover fermions on MILC $N_f = 2+1+1$ ensembles, $m_\pi = 128 - 312$, $m_\pi^{phys} L = 3.9$, 4 lattice spacings, $a = 0.15 - 0.06$ fm

Simultaneous fits to $\mathcal{J} = \mathcal{A}_\mu$ and $\mathcal{P}$ C_{3pt} and C_{2pt} functions (two/three excited states). Three-five source-sink separations $t = 0.8 - 1.4$ fm.

Followed by a three-step procedure:

Q^2 fit to G_A with $k_{max} = 2$.

For 11 reference values of Q^2, extrapolation with respect to m_q, V and a.

At the physical point: fit to 11 Q^2 values with $k_{max} = 2$. Similarly, for $\tilde{G}_P$ and G_P.

Recent works with $m_\pi \to m_\pi^{phys}$, $V \to \infty$, $a \to 0$ limits

[Mainz,2207.03440]: $N_f = 2+1$ $O(a)$-improved Wilson ensembles (CLS), 4 lattice spacings, $a = 0.09 - 0.05$ fm, $m_\pi = 130 - 350$ MeV, $Lm_\pi^{phys} = 4.0$.

G_A only.

Combined excited state and Q^2 fit with $k_{max} = 2$.

$t = 0.2 - 1.4$ fm, 9-17 source-sink separations with ground state fits to the summed ratio $\sum_\tau C_{3pt}(t,\tau)/C_{2pt}(t)$ (summation method [Maiani et al.,Nucl. Phys. B 239 (1987)])

Dependence of the coefficients on m_q, V and a^2 is fitted.

Recent results for $G_A(Q^2)$

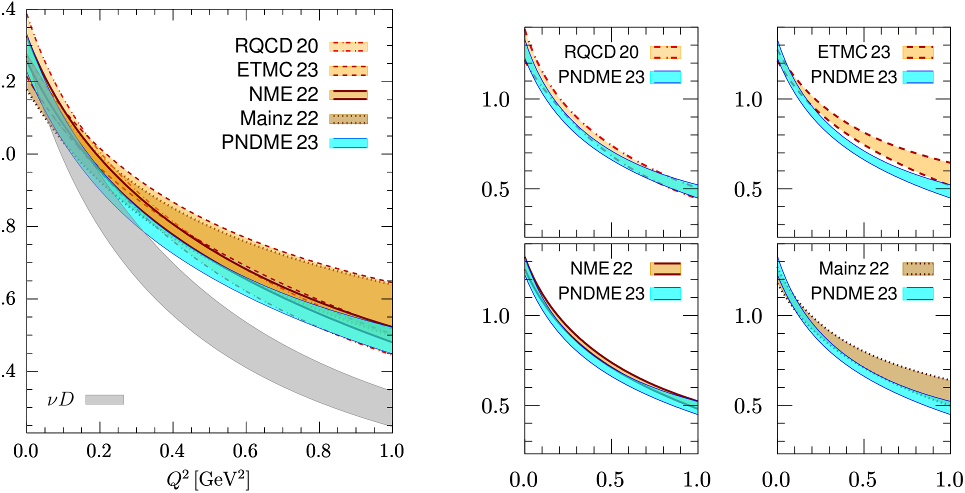

Figures from [Gupta,Lattice 23], νD fit from [Meyer et al.,1603.03048].

Also shown: [NME,2103.05599] clover fermions on MILC $N_f = 2+1+1$ HISQ ensembles, no $m_\pi \to m_\pi^{phys}$, $V \to \infty$, $a \to 0$ limit. Fit $m_\pi = 170 - 285$ MeV, $a = 0.07 - 0.13$ fm data together. Simultaneous fits to $\mathcal{J} = \mathcal{A}_\mu$ and $\mathcal{P}$ C_{3pt} and C_{2pt} functions (one/three excited states). Four-six source-sink separations $t = 0.8 - 1.5$ fm.

Recent results for $G_A(Q^2)$

[Meyer,2301.04616]

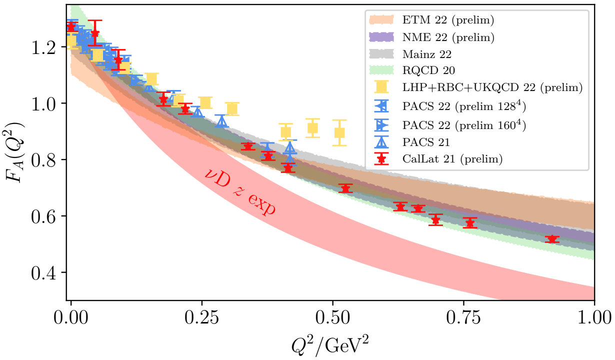

[CalLat,2111.06333], domain wall fermions on MILC $N_f = 2+1+1$ HISQ ensembles, $m_\pi = 130$ MeV, $Lm_\pi = 3.9$, $a = 0.12$ fm. 10 source-sink separations, $t = 0.3 - 1.4$ fm, 3 excited states fitted to C_{3pt}/C_{2pt}.

[PACS,2311.10345], $O(a)$ improved-Wilson $N_f = 2+1$ ensembles, $m_\pi = 138$ MeV, $a = 0.06$ and 0.09 fm. 3 source-sink separations, $t = 0.82 - 1.2$ fm. Ground state fits to ratios.

Recent results for $G_A(Q^2)$

[Tomalak et al.,2307.14920]

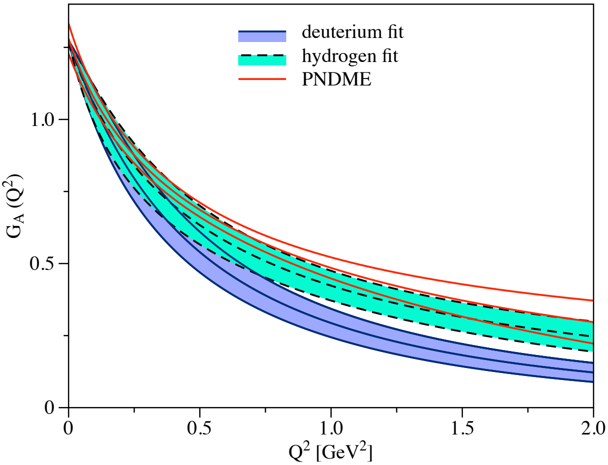

Lattice results are more consistent with MINERvA data.

[MINERva,Nature 614, 48 (2023)]: antineutrino scattering off hydrogen atoms inside hydrocarbon molecules. Monte-Carlo simulations used to remove antineutrino-carbon scattering.

Axial radius: $\langle r^2 \rangle_A$ [fm^2]

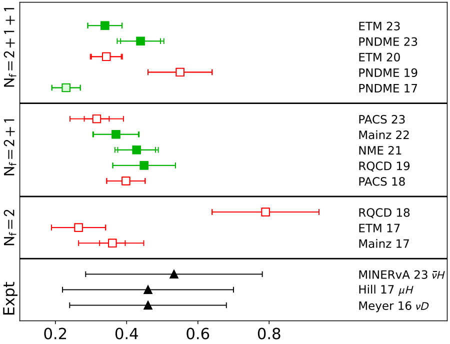

Lattice results and fits to experiment obtained using the z-expansion.

$\tilde{G}_P$ at the muon capture point: g_P^*

$\tilde{G}_P$ not well known from expt: muon capture $\mu^- p \to \nu_\mu n$ gives

$g_P^* = \frac{m_\mu}{2m_N} \tilde{G}_P(Q^2 = 0.88\, m_\mu^2) = 8.06(55)$ [MuCap,1210.6545]

Compatible with pion pole dominance.

[RQCD,1911.13150]

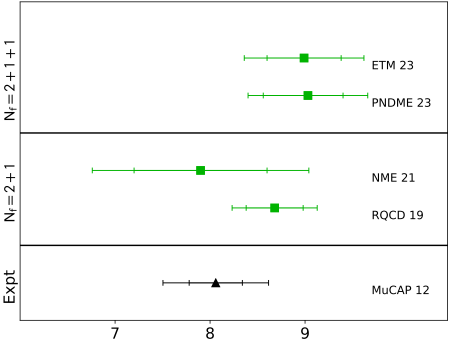

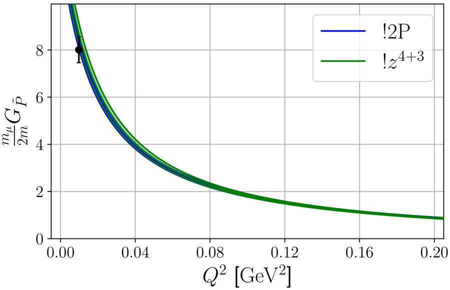

Recap: axial form factors

- ⋆ Many new lattice studies of the axial form factor, with a focus on increasing precision and controlling all the main systematics. General agreement between results.
- ⋆ Constraints, such as the PCAC relation on the form factors, provide an important check on the results. Lattice results now show consistency with the PCAC relation in the continuum limit.
- ⋆ There is very significant excited state contamination of the three-point functions from $N\pi$ states.
- ⋆ Extraction of $\tilde{G}_P$ and G_P are mostly affected, while excited state contamination in the extraction of G_A is "moderate". Consistent with LO ChPT analysis.
- ⋆ Size of the excited state contamination when extracting G_A depends on details of the analysis (choice of nucleon interpolator $\mathcal{N}$, source-sink separations for C_{3pt}, m_π, L, ...). Still needs to be considered carefully, for precision results.
- ⋆ Lattice results now reproduce the expt. value for g_P^*. Pion pole dominance in $\tilde{G}_P$ is also found to hold on a few percent level.

Toward N to $N\pi$ matrix elements

Neutrino scattering above the pion-production threshold ($E_\nu \sim 1 - 10$ GeV):

$\star$ $N \to N\pi$ transition matrix elements: $N \to \Delta(1232), N^*$ resonances for vector and axial currents.

$\star$ Straightforward if m_π is large enough for the resonance to be stable, e.g. [ETMC,0710.4621,0706.3011] ($N \to \Delta$), [Lin, Cohen,1108.2528] ($N \to$ Roper) and earlier $N_f = 0$ works.

$\star$ $N \to$ resonance requires finite volume formalism for $N\pi \to N\pi$ scattering as well as $N \to N\pi$ [Bernard et al.,1205.4642], [Agadjanov et al.,1405.3476], [Briceno, Hansen,1502.04314].

$\star$ Elastic $N\pi$ scattering in $I = 1/2$ and $3/2$, see e.g. [Lang et al.,1610.01422], [Anderson et al.,1710.01557], [Bulava et al.,2208.03867], [ETMC,2307.12846].

Toward N to $N\pi$ matrix elements

Computing $N \to N\pi$ matrix elements:

[Barca et al.,2211.12278] $N_f = 3$ $(m_\ell = m_s)$ $m_\pi = 420$ MeV, $a = 0.098$ fm.

[ETMC,2312.15737] $N_f = 2+1+1$ $m_\pi = 346$ MeV, $a = 0.095$ fm, $N_f = 2$ $m_\pi = 131$ MeV, $a = 0.094$ fm.

⋆ First step: evaluating GEVP improved $N \to N$ axial form factors with reduced excited state contributions.

⋆ Next step: $N \to N\pi$ matrix elements from the GEVP.

GEVP for the two-point functions

[Barca et al.,2211.12278]

Matrix of correlation functions: $C_{ij}(\vec{p},t) = \langle O_i(\vec{p},t)\overline{O}_j(\vec{p},0)\rangle$, $O_i \in \{O_{3q}, O_{5q}\}$.

$O_{3q,5q}$ must be projected onto the relevant lattice irreducible representation to give spin 1/2:
$(\vec{p}=\vec{0})$ G_1^+ of O_h , $(\vec{p}\neq\vec{0})$ G_1 of the little group C_{4v}.

Similarly, for isospin:
e.g. for the neutron $(I=-I_z=1/2)$ $O^n_{5q} = -\frac{1}{\sqrt{3}}O^n_{3q}O^{\pi^0}_{\bar{q}q} + \sqrt{\frac{2}{3}}O^p_{3q}O^{\pi^-}_{\bar{q}q}$

GEVP: $C(t)V(t,t_0) = C(t_0)V(t,t_0)\Lambda(t,t_0)$,
$V(t,t_0) = (v^1(t,t_0), v^2(t,t_0))$

$\Lambda(t,t_0) = \mathrm{diag}(\lambda^1(t,t_0), \lambda^2(t,t_0))$,
$\boldsymbol{\lambda^\alpha(t,t_0) \approx d_\alpha(t_0)e^{-E_\alpha t}}$

Setup: $t_0 = 2a$, $|\vec{p}| = 2\pi/L$
(top) $\boldsymbol{O_{5q}(\vec{0})} = O_{3q}(\vec{p})O_{\bar{q}q}(-\vec{p})$
(bottom) $\boldsymbol{O_{5q}(\vec{p})} = O_{3q}(\vec{0})O_{\bar{q}q}(\vec{p})$

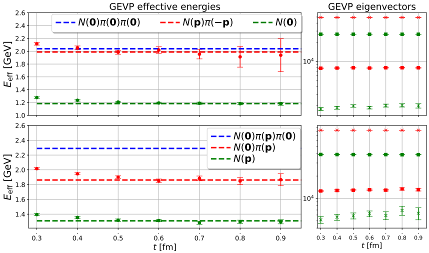

Note $E_2 \approx E_N + E_\pi$ and $v^1_i\overline{O}_i|\Omega\rangle \approx |N\rangle$, $v^2_i\overline{O}_i|\Omega\rangle \approx |N\pi\rangle$.

Little $N\pi$ in $\overline{O}_{3q}|\Omega\rangle \Rightarrow N\pi$ not visible in $\langle O_{3q}(\vec{p},t)\overline{O}_{3q}(\vec{p},0)\rangle$.

GEVP-projected correlation functions

Use eigenvectors $v^{1,2} \sim v^{N,N\pi}$ to obtain GEVP-improved two- and three-point functions for $\boldsymbol{\alpha, \beta \in \{N, N\pi\}}$:

$$C_{2pt}^{\alpha}(\vec{p}, t) = v_i^{\alpha}(\vec{p}, t; t_0) C_{ij}(\vec{p}, t) v_j^{\alpha}(\vec{p}, t; t_0)$$
$$C_{3pt}^{\alpha,\beta}(\vec{p}, t, \vec{q}, \tau; P_k; \mathcal{J}) = v_i^{\alpha}(\vec{p}', t; t_0) C_{ij}^{3pt}(\vec{p}, t, \vec{q}, \tau; P_k; \mathcal{J}) v_j^{\beta}(\vec{p}, t; t_0)$$

$|v_2^N|$ and $|v_1^{N\pi}|$ are small. However, there is an enhancement of $N \xrightarrow{\mathcal{J}} N\pi$.

Neglect $\sim |v_2^N|^2$ **(small)^2 terms**, i.e. $\langle O_{5q} \mathcal{J} \overline{O}_{5q} \rangle$ is not computed.

Improved nucleon matrix elements can be obtained from

$$\boldsymbol{R^{k,\mathcal{J}}(\vec{p}\prime, t; \vec{q}, \tau)^{NN}} = \frac{C_{3pt}^{k,\mathcal{J}}(\vec{p}', t; \vec{q}, \tau)^{NN}}{C_{2pt}(\mathbf{p}', t)^N} \sqrt{\frac{C_{2pt}(\mathbf{p}', \tau)^N \; C_{2pt}(\mathbf{p}', t)^N \; C_{2pt}(\mathbf{p}, t-\tau)^N}{C_{2pt}(\mathbf{p}, \tau)^N \; C_{2pt}(\mathbf{p}, t)^N \; C_{2pt}(\mathbf{p}', t-\tau)^N}} \,.$$

Wick contractions $p \to p\pi^-$

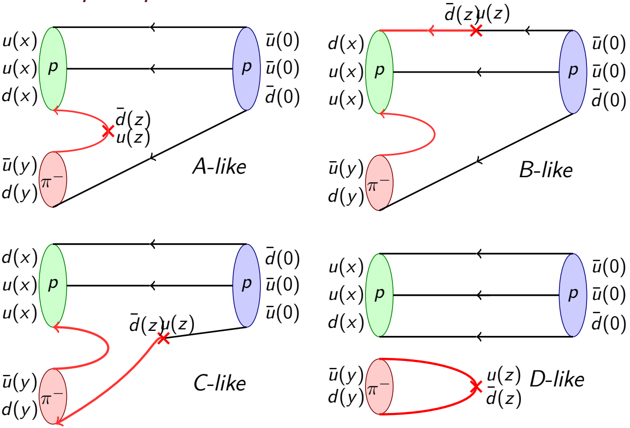

$p \to n\pi^0$: A, B, C diagrams but no D diagram.

Largest contribution from the *D* diagram: we find D diagram

$$\approx C^N_{2pt}(\vec{p}'_N, t; \vec{p}, 0) \times C^\pi_{2pt}(\vec{p}'_\pi, t; \vec{q}, \tau) \overset{\mathcal{J}=\mathcal{A}_\mu}{\propto} \delta_{\vec{p}'_N,\vec{p}}\delta_{\vec{p}'_\pi \vec{q}} q_\mu e^{-E_N t} e^{-E_\pi(t-\tau)}.$$

Two-point functions: same topologies, current at $\tau \longrightarrow$ smeared pion interpolator at $\tau = 0$.

A, B, C diagrams evaluated using the sequential source method. D diagram, one-end trick [Foster, Michael,hep-lat/9810021] for the pion part.

$R^{k,\mathcal{J}}(\vec{p}\prime, t; \vec{q}, \tau)^{NN}$ with momentum transfer

Set up:

Source (left): $\vec{p} = -\vec{q} = \hat{e}_z 2\pi/L$, sink (right): $\vec{p}' = 0$.

Source: most excitations removed, sink (at rest): some excitations remain.

$R^{\mathcal{A}_4} \propto G_A, \tilde{G}_P + \ldots$

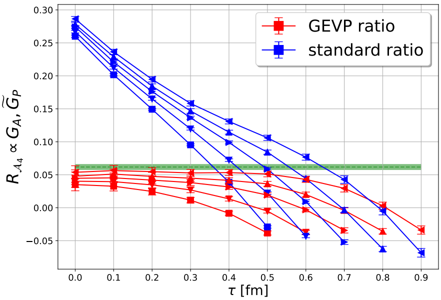

$R^{\mathcal{P}} \propto G_P + \ldots$

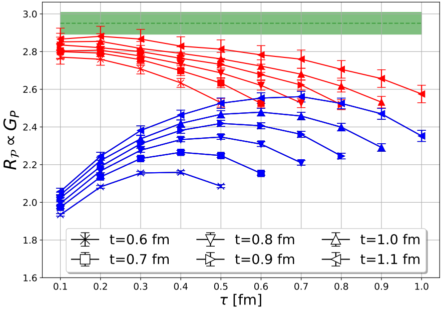

Blue: Large contributions from $\langle N(\vec{0})\pi(\hat{e}_z)|\mathcal{A}_4|N(\vec{0})\rangle$ and $\langle N(\hat{e}_z)|\mathcal{A}_4|N(\hat{e}_z)\pi(-\hat{e}_z)\rangle$ due to the D diagram etc.

Green bands: ground state matrix element obtained from fit **M2**, see below.

PCAC and PPD relations

$N_f = 3$ ($m_\ell = m_s$) $m_\pi = 420$ MeV, $a = 0.098$ fm

GEVP-improved $N \to N$ form factors consistent with PCAC and PPD relations up to around 10%.

Note: the axial form factor G_A does not change significantly, see ETMC results below.

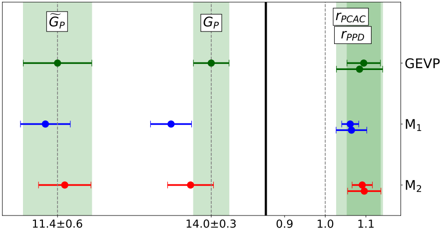

Fitting analyses of $\langle O_{3q} \mathcal{J} \overline{O}_{3q} \rangle$ correlation functions also give consistent results:

M1: fit used in [RQCD,1911.13150], guided by ChPT with mass gap to 1st excited state fixed with a prior to $E_{N\pi}$.

M2: combined one excited state fit to three- to two-point function ratios for $\mathcal{J} = \mathcal{A}_\mu$ and $\mathcal{P}$, similar to [Jang et al.,1905.06470] and [ETMC,2309.05774].

$N \to N\pi$ transition matrix elements from the GEVP

Setup: $\vec{q} = \vec{0}$, $\vec{p}' = \vec{p} = \hat{e}_z \times 2\pi/L$, $\boldsymbol{Q^2 = m_\pi^2}$.

Only moderate excited state contributions to $R^{\mathcal{P},\mathcal{A}_4}(\vec{p}, t; \vec{0}, \tau)^{N\pi N}$.

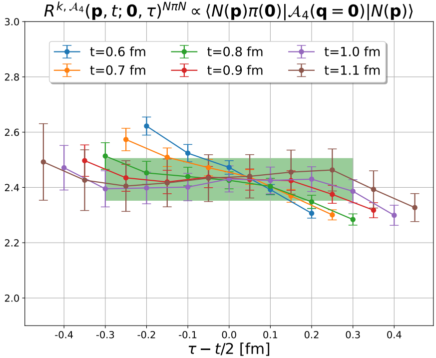

Note that the Lorentz decomposition of the $N \to N\pi$ matrix elements is different to that for $N \to N$.

GEVP improved form factors from ETMC

[ETMC,2312.15737] Effective energies of eigenvalues and eigenvector for the lowest eigenenergy.

(Left) $N_f = 2+1+1$, $m_\pi = 346$ MeV, $a = 0.095$ fm
(Right) $N_f = 2$, $\boldsymbol{m_\pi = 131}$ **MeV**, $a = 0.094$ fm.

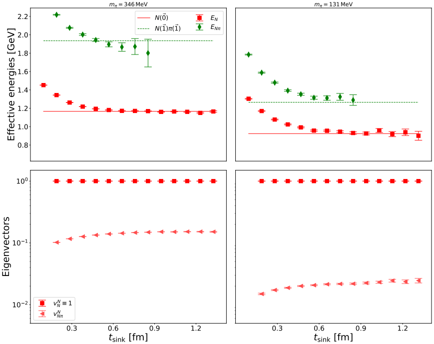

Omitted: additional diagrams involving pion loops arising from the breaking of isospin symmetry with twisted mass fermions. Also $\langle O_{5q} \mathcal{J} O_{5q} \rangle$ correlation functions.

GEVP improved form factors from ETMC

Forward limit: no signifiant change in the excited state contributions when using GEVP improved three-point functions to extract g_A

With momentum transfer: $|\vec{q}| = 2\pi/L$
Left: $m_\pi = 346$ MeV, $Q^2 = 0.283$ GeV^2
Right: $m_\pi = 131$ MeV, $Q^2 = 0.074$ GeV^2

$\bar{G}_5^{u-d}$ denotes the form factor extracted with $\mathcal{J} = \mathcal{P}$ with the pole removed:

$$\bar{G}_5^{u-d} = \frac{m_\pi^2 + Q^2}{F_\pi m_\pi^2} m_q G_5$$

Similarly for $\bar{G}_{P,i}^{u-d}$ and $\bar{G}_{P,t}^{u-d}$ extracted with $\mathcal{J} = \mathcal{A}_i$ and $\mathcal{J} = \mathcal{A}_4$, respectively.

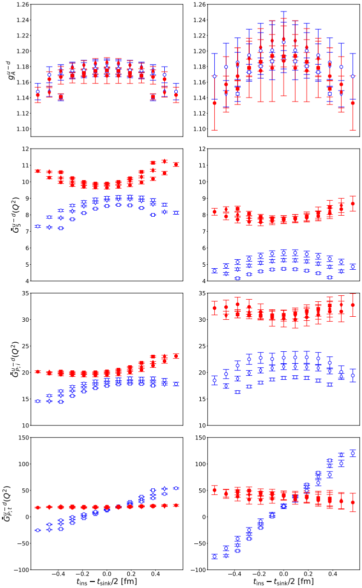

Summary and outlook

- ⋆ First steps towards computing $N \to N\pi$ matrix elements relevant for $N \to \Delta$, ... transitions have been made.
- ⋆ Large $N\pi$ contributions to the axial and pseudoscalar three-point functions can be removed via the GEVP for $m_\pi \sim 420$ MeV down to 131 MeV.
- ⋆ Fitting analyses to $\langle O_{3q} \mathcal{J} O_{3q} \rangle$ correlation functions that account for $N\pi$ contributions agree with GEVP results for $\tilde{G}_P$ and G_P. (Limited test at $m_\pi = 420$ MeV).
- ⋆ No significant change in g_A.

More work to be done:

- ⋆ $N \to N\pi$: extended basis of operators for range of $\vec{p}$, implement the finite volume formalism.
- ⋆ G_A: how to deal with the "moderate" excited state contamination? Control over other systematics.
- ⋆ ...